

Disorder-Induced Floquet Topological Insulators

Paraj Titum,¹ Netanel H. Lindner,^{1,2} Mikael C. Rechtsman,² and Gil Refael¹

¹*Department of Physics, Institute of Quantum Information and Matter, Caltech, Pasadena, California 91125, USA*

²*Department of Physics, Technion-Israel Institute of Technology, Haifa 32000, Israel*

(Received 19 March 2014; published 4 February 2015)

We investigate the possibility of realizing a disorder-induced topological Floquet spectrum in two-dimensional periodically driven systems. Such a state would be a dynamical realization of the topological Anderson insulator. We establish that a disorder-induced trivial-to-topological transition indeed occurs, and characterize it by computing the disorder averaged Bott index, suitably defined for the time-dependent system. The presence of edge states in the topological state is confirmed by exact numerical time evolution of wave packets on the edge of the system. We consider the optimal driving regime for experimentally observing the Floquet topological Anderson insulator, and discuss its possible realization in photonic lattices.

DOI: 10.1103/PhysRevLett.114.056801

PACS numbers: 73.20.-r, 03.65.Vf, 71.10.Pm, 71.23.An

Topological states have been an ongoing fascination in condensed matter and recently led to the prediction [1–3] and realization [4–6] of various topological phases, including topological insulators (TIs). TIs possess extraordinary properties (gapless edge states [7,8], topological excitations [9]) and have a myriad of potential applications from spintronics to topological quantum computation [10]. One method to generate topological states is via periodic driving of a topologically trivial system out of equilibrium. These so-called Floquet topological insulators (FTIs) might be obtained by irradiating ordinary semiconductors with a spin-orbit interaction [11,12], or graphenelike systems [13–16]; analogues in superconducting systems have also been proposed [17,18]. Topological phases thus obtained introduce new parameters for controlling the phase, such as the frequency and intensity of the drive. Also, while FTIs have gapless edge states (just as topological insulators do), they exhibit phases with no analog in equilibrium systems [19,20]. Remarkably, topological Floquet spectra were recently experimentally realized in artificial photonic lattices where edge transport was observed [21], as well as in the solid state [22]. The tunability of photonic systems is conducive to exploring a variety of effects, including the influence of controlled disorder.

Here, we are interested in the interplay of disorder and topological behavior. In two-dimensional TIs, it has been shown [23] that ballistic edge modes are robust to disorder as long as there is a bulk mobility gap. In contrast, disorder completely localizes the states of trivial non-interacting (and spinless) 2D systems. In the presence of strong spin-orbit coupling, however, disorder can induce a phase transition from a trivial to a topological Anderson insulator (TAI) phase, which exhibits quantized conductance at finite disorder strengths. TAIs were predicted in electronic models [24–27], but have not been observed experimentally.

Can disorder induce topological phases in trivial periodically driven systems? Naively, we would think that disorder would destroy the conditions that give rise to Floquet topological phases. Nevertheless, we find concrete examples where disorder induces a topological phase. Here we investigate such transitions in driven systems, and describe their unique properties. The model we consider is a graphenelike lattice subject to circularly polarized light, with a staggered potential and on-site disorder. We obtain the phase diagram as a function of disorder strength by calculating the disorder-averaged bulk topological invariant viz., the Bott index. The time evolution of wave packets reveals gapless edge modes in the topological phase. As we explain below, our model is especially appealing as it is amenable to experimental realization in photonic lattices.

Our starting point is the tight binding Hamiltonian of a honeycomb lattice subject to circularly polarized light,

$$H_0(t) = \sum_{\langle i\alpha, j\alpha' \rangle} t_1 e^{iA_{ij}} c_{i\alpha}^\dagger c_{j\alpha'} + M \sigma_{\alpha\alpha}^z c_{i\alpha}^\dagger c_{i\alpha}, \quad (1a)$$

$$H(t) = H_0(t) + U_{\text{dis}}, \quad (1b)$$

where $\alpha \in \{1, 2\}$ indicates sublattices A and B , $A_{ij} = (e/\hbar)\mathbf{A}(t) \cdot (\mathbf{r}_i - \mathbf{r}_j)$ and $\mathbf{A} = A_0(\sin(\Omega t), \cos(\Omega t))$ is the vector potential for the incident circularly polarized light of frequency Ω . We consider nearest neighbor hopping with magnitude t_1 . σ^z is the Pauli matrix, and M is the staggered sublattice potential. $H_0(t)$ represents the clean limit for the system and $H(t)$ is the full Hamiltonian with U_{dis} the disorder potential. The disorder is chosen as an on-site chemical potential, and is diagonal in the real-space representation. We choose the natural system of units $\hbar = e = c = 1$ and set lattice spacing $a = 1$. The bandwidth of the time-independent part of $H_0(t)$ is W . As we explain below, the model of Eq. (1) can be directly

implemented in the photonic lattice realization considered by Rechtsman *et al.* [21].

The idea behind our construction of a Floquet topological Anderson phase is the following. A honeycomb lattice with a staggered potential, Eq. (1), has a gap M at both Dirac cones. A periodic drive alone also induces a gap, with masses of opposite sign at the two Dirac cones. To second order, this gap is simply $\pm A_0^2 v_F^2 / \Omega$, for the K and K' points. Thus, the drive induces effectively a Haldane model [28], and yields an example of a Floquet topological phase [13,14]. For weak and high-frequency ($\Omega \gg t_1$) drives, where perturbation theory is valid, the drive and the staggering compete. Thus, the system is topological when $M < v_F^2 A_0^2 / \Omega$, with a Chern number $|C_F| = 1$, and trivial otherwise. The key is the effect of disorder: it diminishes a band gap induced by the drive, but even more strongly it suppresses the staggering. Starting from the trivial phase, $M > v_F^2 A_0^2 / \Omega$, an increase in disorder may reverse this balance, and induce a topological phase (for a static analog, see Ref. [13]). In [29], we provide a Born-approximation analysis of the disorder effects on the two gaps in the static limit.

The explanation above, however, relies on a weak, high-frequency drive, which effectively produces a static perturbation. It does not capture the scenario in which the topological properties of the time-dependent system are a result of a resonance, connecting states of the original bulk band structure. In addition, we find that it is necessary to consider strong driving in order to observe the disorder induced topological phase. Below, we will establish the existence of the Floquet topological Anderson phase beyond the limit of a weak, high-frequency drive. We will consider strong periodic drives, and will analyze two distinct frequency regimes: the high-frequency regime ($\Omega > W$), and the low-frequency ($\Omega < W$) regime in which resonances occur within the band structure. We will compare the two regimes and show that both of them exhibit a disorder-induced FTAI phase.

First, let us transform the problem defined in Eq. (1) into a time-independent Hamiltonian. We define H^F as follows:

$$H_{nm}^F = n\Omega\delta_{nm} + \int_0^{2\pi/\Omega} dt e^{i\Omega(n-m)t} H(t). \quad (2)$$

The ‘‘Floquet’’ indices n (and m) refer to replicas of the Hilbert space. The eigenstates of H^F are the quasienergies (ϵ), which are periodic in a quasienergy ‘‘Brillouin’’ zone with period Ω . We set the boundaries of this zone at $\pm\Omega/2$. The off-diagonal terms (in Floquet indices) of H_{nm}^F emerge from the hopping term in Eq. (1), $(H_0)_{ij} = t_1 \exp(iA_0 \cos(\Omega t + \phi_{ij}))$, where (i, j) indicates hopping from site i to j and $\phi_{ij} = \pm(\pi/3)$ or 0. Therefore, $(H_{m,m+n}^F)_{ij} = t_1 i^n J_n(A_0) \exp(i\phi_{ij})$, where $J_n(A_0)$ are the Bessel functions of the first kind. Here, to efficiently use exact diagonalization, we neglect $H_{m,m+n}^F = 0$ for $n \geq 2$.

We also truncate $(H_F)_{nm}$, such that the Floquet indices obey $|n|, |m| \leq n_{\max}$, with n_{\max} determined through convergence tests. The typical quasienergy spectrum of our model is given in Figs. 1(b) and 1(c), where we have defined a renormalized hopping, $\tilde{t} = t_1 J_0(A_0)$.

The quasienergy band structure encodes the topological properties of time-periodic Hamiltonians. While noninteracting equilibrium 2D Hamiltonians with broken time-reversal symmetry are classified by the Chern number, periodically driven systems require a more general topological invariant—the winding number—which counts the number of edge states at a particular quasienergy [20]. In disordered time-independent systems, the disorder-averaged Chern number is the Bott index, as defined by Hastings and Loring [32]. For our periodically driven model, the disorder-averaged winding number is calculated using the Bott indices obtained from the eigenvalues and eigenvectors of H_F , defined in Eq. (2), and truncated to a finite number of replicas (for full details, see [29]). The Bott index at a particular quasienergy $C_b(\epsilon)$ for the truncated H_F is the number of edge states at that quasienergy [20]. Also, the Chern number of a quasienergy band is simply the difference in the Bott indices at the band edges.

Let us first consider the case of $\Omega > W$ without resonances. The clean system forms a trivial insulator, with its quasienergy spectrum shown in Fig. 1(c). The Bott index C_b as a function of disorder strength U_0 and quasienergy is shown in Fig. 2(a). At very weak disorder, the index $C_b(\epsilon = 0) = 0$ in the quasienergy gap, and it is not quantized at other quasienergies, indicating a trivial phase. A topological phase emerges as disorder increases, and is manifested by the Bott index becoming one: $C_b(0) \sim 1$. This phase is induced by both disorder and

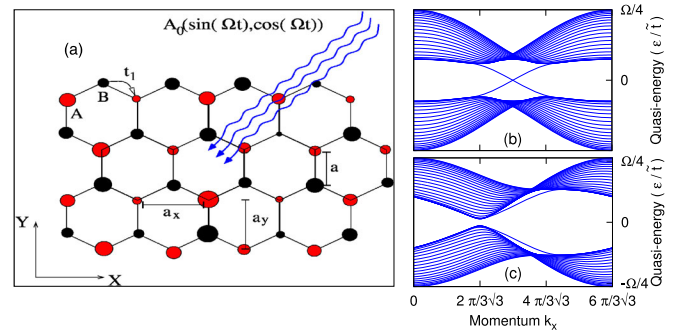


FIG. 1 (color online). (a) Schematic representation of the system indicating uniformly disordered graphene in the presence of a staggered mass potential and a circularly polarized light. Red-black coloring indicates the staggered mass in the sublattices A and B, and the variable radius of the disorder potential. (b) The Floquet band structure for the pure system with parameters, $A_0 = 1.43$, $M = 0$, and $\Omega/\tilde{t} = 12$. The system is topological and supports edge states. The bulk gap is given by the topological mass $\Delta/\tilde{t} \approx 0.75$. (c) A trivial Floquet band structure. All parameters are the same as (b) except $M/\tilde{t} = 0.85$.

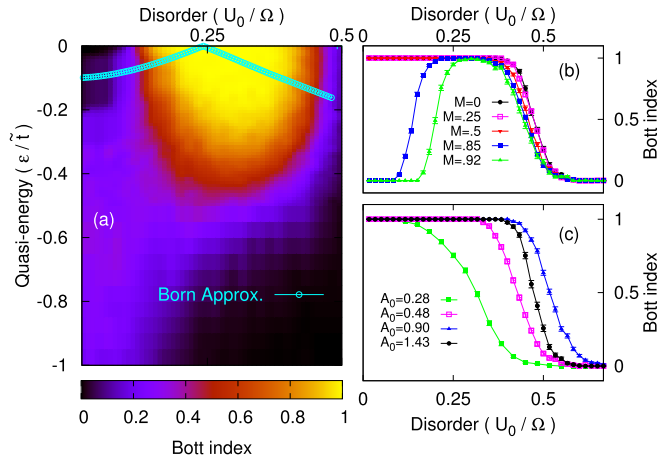


FIG. 2 (color online). (a) The Bott index C_b (in color) as a function of the quasienergy and the disorder strength. Edge states are observed in the region where $C_b(0) = 1$. The quasienergy gap, in the Born approximation, is shown (cyan) as a function of disorder. The system parameters are $A_0 = 1.43$, $M/\tilde{t} = 0.85$ and the size is $(L_x, L_y) = (30, 30)$. (b) C_b as a function of disorder for different staggered masses $M/\tilde{t} = 0, 0.5, 0.85, 1$ at quasienergy $\epsilon = 0$ keeping t_1 and A_0 the same as (a). (c) C_b as a function of disorder for different driving strengths $A_0 = 0.28, 0.48, 0.90$, and 1.43 , keeping fixed t_1 and $M/t_1 = 0$. We have set $\Omega/t_1 = 12J_0(1.43)$.

drive, and, therefore, we identify it as a Floquet topological Anderson insulator (FTAI). As expected, varying M while keeping the drive strength fixed shifts the position of the trivial-topological transition [see Fig. 2(b)]. A qualitative description of this transition is provided by the disorder-averaged Born approximation [29]. Even though this approximation [Fig. 2(a)] captures this basic physics of the transition, it overestimates the exact point of the transition.

At disorder strengths that are considerably larger than the transition point, the FTAI phase is destroyed and there is localization at all quasienergies. This transition is insensitive to the staggered potential strength, as is evident from Fig. 2(b); however, it depends on the drive strength [see Fig. 2(c)]. To observe the FTAI, the trivial-to-topological transition must occur well before the localization transition. Thus we consider the effects of strong driving (where $A_0 \sim 1$). As discussed in [29], the finite-size dependence of the Bott index as a function of quasienergy in the topological phase is in agreement with the presence of an extended state in the bulk. The topological phase is protected against disorder if there is a “mobility gap” in the spectrum, and some states are delocalized.

Next we numerically examine the existence of edge states as a diagnostic for topological phases. The time-evolution operator for $H(t)$ is obtained in discrete time steps δt using a split-operator decomposition. The honeycomb lattice [Fig. 1(a)] is considered in a cylindrical geometry, with periodic boundary conditions along X

and open ones along Y [see Fig. 3(a)]. Initializing with a δ -function wave packet at $\mathbf{r}_0 \equiv (x_0, y_0)$, the Green’s function $G(\mathbf{r}, \mathbf{r}_0, t)$ is obtained from the time-evolution operator, $U(t, 0)$. An evolution for N time periods ($T = 2\pi/\Omega$) yields $G_N(\mathbf{r}, \mathbf{r}_0, NT) = \langle \mathbf{r} | U(t = NT, 0) | \mathbf{r}_0 \rangle$. The initial position \mathbf{r}_0 is chosen to probe edge or bulk. Compared to the analysis by exact diagonalization of H^F , in this method we do not need approximations, and large system sizes are accessible.

The propagator $G_N(\mathbf{r}, \mathbf{r}_0, NT)$ is the Floquet Green’s function obtained from H^F [29]. So, the quasienergy eigenvalues and eigenstates are analyzed by Fourier transforming the Green’s function in time, $G_N(\mathbf{r}, \mathbf{r}_0, \epsilon)$. With disorder we calculate $g_N(\mathbf{r}, \mathbf{r}_0, \epsilon) = \langle |G_N(\mathbf{r}, \mathbf{r}_0, \epsilon)|^2 \rangle$, where $\langle \cdot \rangle$ indicates disorder averaging. The extended or localized nature of the states at quasienergy ϵ is given by the spread of g_N defined as $\lambda_x(N)$, and $\lambda_y(N)$, along X and Y directions, respectively.

The time evolution is carried out for a system with $A_0 = 1.434$, $M/\tilde{t} = 0.85$, $U_0/\tilde{t} = 3.5$, and $\Omega/\tilde{t} = 12$. These parameters correspond to a FTAI and, thus we expect ballistic edge states at $\epsilon = 0$. The initial wave packets are chosen in the A sublattice, on the two edges [cases (I) and (III)], and the bulk (II), as shown in Fig. 3(a). After evolution for N cycles, $g_N(\mathbf{r}, \mathbf{r}_0, 0)$, for all three cases is shown in Fig. 3(c). For cases (I) and (III), g is extended along X and localized in Y , indicating the presence of an

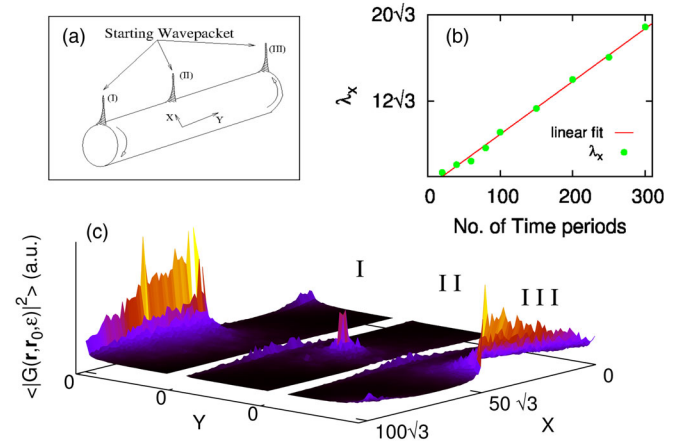


FIG. 3 (color online). (a) The cylindrical geometry for the time evolution of a starting δ -function wave packet. Cases (I), (II) and (III) have the starting positions, $\mathbf{r}_0 \equiv (x_0, y_0)$ in the A sublattice at the left edge, bulk and right edge with $y_0/a_y = 0, N_y/2 - 1$ and N_y respectively. In all the cases, we fix $x_0/a_x = N_x/2$. (b) The spread of $g_N(\mathbf{r}, \mathbf{r}_0, 0)$ as a function of total time of evolution $T_f = NT$ along the X direction, for \mathbf{r}_0 corresponding to case (I). $\lambda_x(N)$ grows linearly, with a velocity $v_{\text{edge}} = (0.09 \pm 0.001)a/T$. (c) $g_N = \langle |G_N(\mathbf{r}, \mathbf{r}_0, \epsilon = 0)|^2 \rangle$ in real space as a function of \mathbf{r} , for the three cases, with $N = 300$ and averaged over 400 realizations of disorder. Each sublattice has $N_x \times N_y = 100 \times 30$ points. The system parameters are $A_0 = 1.43$, and $M/\tilde{t} = 0.85$.

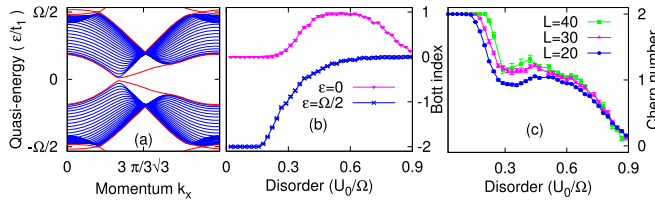


FIG. 4 (color online). (a) Band structure for the case of a single resonance. Edge-states (shown in red) are observed at the two bulk band gaps at quasi-energies $\epsilon/t_1 = 0$ and $\Omega/2$. The gap at $\epsilon = 0$ is made trivial by a staggered mass. The system parameters are $A_0 = 0.75$, $M/t_1 = 0.3$, and $\Omega/t_1 = 9/2$. (b) Disorder-averaged Bott index at a particular quasi-energy gap, $C_b(0)$ (magenta) and $C_b(\Omega/2)$ (blue). The Floquet Hamiltonian is truncated after 9 Floquet bands. System size is $(L_x, L_y) = (30, 30)$. (c) Disorder-averaged Chern number, $C_F = C_b(0) - C_b(\Omega/2)$, of a single Floquet band between $\epsilon = -\Omega/2$ and $\epsilon = 0$.

edge state. The decay of g_N along X after some finite distance is due to finite time evolution. The chiral nature of the edge states are also revealed by the direction in which $g_N(\mathbf{r}, \mathbf{r}_0, \epsilon)$ evolves as a function of N . Figure 3(b) shows that $\lambda_x(N)$ increases linearly with time of evolution N , indicating that the edge states are ballistic and do not backscatter from impurities. In contrast, bulk states are diffusive in nature until Anderson localization sets in. A finite amplitude is observed on the edge when starting with a bulk wave packet because the bulk localization length is larger than the width of the system, indicating an overlap of the edge state wave function with the initial wave packet. We have shown the presence of protected edge states. This confirms the existence of the FTAI.

This novel phase persists even when there is a resonance within the band structure ($\Omega < W$). There, a transition occurs between an FTI phase and the disorder-induced FTAI phase. Furthermore, the FTAI phase in this case cannot be understood using perturbative arguments since the resonance alters the topological nature of all the Floquet bands in the problem [29]. Figure 4(a) shows the quasi-energy spectrum of the clean system. The gap at the resonance, $\epsilon = \Omega/2$ is topological with $|C_b(\Omega/2)| = 2$ and, thus, supports two edge states. The gap at the Dirac points is trivial, $|C_b(0)| = 0$, since the staggered mass M still dominates over the effect of the drive near $\epsilon = 0$. Figure 4(b) shows two transitions as disorder is increased. A topological-to-trivial transition removes the edge states in the gap at the resonance ($\epsilon = \pm\Omega/2$). Another transition induces topological edge states at $\epsilon = 0$. From the finite sizes investigated, the topological to trivial transition at $\epsilon = \Omega/2$ happens initially and is unrelated to the transition at $\epsilon = 0$. Finally, disorder becomes strong enough to localize the entire band, as in the high-frequency case. The Chern number of the band between these two quasi-energies $C_F = C_b(0) - C_b(\Omega/2)$ changes from $|C_F| = 2$ to $|C_F| = 1$, and then to $|C_F| = 0$ [Fig. 4(c)]. The

intermediate regime, with $|C_F| = 1$, is again identified as a FTAI—it is a topological state that requires both disorder and a periodic drive. The fact that this phase exists even in a system which is nonperturbatively affected by the periodic drive indicates the universality and robustness of the FTAI.

This FTAI phase is directly amenable to experimental observation. Recently a topological band structure was experimentally demonstrated [21] in a structure composed of an array of coupled waveguides (a “photonic lattice”). There, the diffraction of light is governed by the paraxial Schrödinger equation, wherein the spatial coordinate along the waveguide axis acts as a time coordinate. The guided modes of the waveguides are analogous to atomic orbitals, and thus the diffraction is governed by a tight-binding model. By fabricating the waveguides in a helical fashion, z -reversal symmetry is broken, resulting in a photonic Floquet topological insulator [11], with topologically protected edge states.

The same system may give a realization of Eq. (1) and the proposed FTAI phase. The gauge field A_0 in the photonic system is determined by the helix radius and period. The sublattice potential M and on-site disorder U_0 may be implemented by fabricating waveguides of different refractive indices, which is straightforwardly done in the laser-writing fabrication process [33]. Since each waveguide can be fabricated with a specified refractive index, the mass M and disorder strength U_0 can be tuned entirely independently. In the Supplemental Material [29], we fully discuss the relevant experimental parameters in the photonic lattice setup and demonstrate that the data we have presented here (shown in Figs. 2–4) are entirely amenable to experiment. The topological transition may be probed by measuring transmission through the photonic lattice for samples of different disorder strengths. For small disorder, the presence of a bulk band gap will give rise to zero transmission through the sample. For disorder strengths above the transition, the presence of edge states in the band gap will allow transmission through the sample: a direct experimental observable. Therefore, the FTAI phase may be implemented using an optical wave function in a photonic crystal structure, as opposed to an electronic wave function in a condensed matter system.

In summary, we have established the existence of a disorder-induced Floquet topological insulator phase. Starting from a clean system that is trivial even in the presence of time-periodic driving, disorder renormalizes the parameters of the Hamiltonian to make the system topological. Experimentally, the parameters are in a range that can be achieved in a photonic lattice, and this could be a first experimental realization of the topological Anderson insulators.

We thank Kun W. Kim, Shu-Ping Lee, Victor Chua, and S. M. Bhattacharjee for illuminating discussions. This work was funded by the NSF Grant No. DMR-1410435, the Packard Foundation, and by the Institute for Quantum

Information and Matter, an NSF Physics Frontiers Center with support of the Gordon and Betty Moore Foundation. N. L. acknowledges financial support by the Bi-National Science Foundation, and by ICore: the Israeli Excellence Center “Circle of Light.”

-
- [1] B. A. Bernevig, T. L. Hughes, and S.-C. Zhang, *Science* **314**, 1757 (2006).
- [2] C. L. Kane and E. J. Mele, *Phys. Rev. Lett.* **95**, 146802 (2005).
- [3] L. Fu, C. L. Kane, and E. J. Mele, *Phys. Rev. Lett.* **98**, 106803 (2007).
- [4] M. König, S. Wiedmann, C. Brune, A. Roth, H. Buhmann, L. W. Molenkamp, X.-L. Qi, and S.-C. Zhang, *Science* **318**, 766 (2007).
- [5] D. Hsieh, D. Qian, L. Wray, Y. Xia, Y. S. Hor, R. J. Cava, and M. Z. Hasan, *Nature (London)* **452**, 970 (2008).
- [6] A. Roth, C. Brune, H. Buhmann, L. W. Molenkamp, J. Maciejko, X.-L. Qi, and S.-C. Zhang, *Science* **325**, 294 (2009).
- [7] M. König, H. Buhmann, L. W. Molenkamp, T. Hughes, C.-X. Liu, X.-L. Qi, and S.-C. Zhang, *J. Phys. Soc. Jpn.* **77**, 031007 (2008).
- [8] B. Zhou, H.-Z. Lu, R.-L. Chu, S.-Q. Shen, and Q. Niu, *Phys. Rev. Lett.* **101**, 246807 (2008).
- [9] X.-L. Qi, T. L. Hughes, and S.-C. Zhang, *Nat. Phys.* **4**, 273 (2008).
- [10] C. Nayak, S. H. Simon, A. Stern, M. Freedman, and S. Das Sarma, *Rev. Mod. Phys.* **80**, 1083 (2008).
- [11] N. H. Lindner, G. Refael, and V. Galitski, *Nat. Phys.* **7**, 490 (2011).
- [12] N. H. Lindner, D. L. Bergman, G. Refael, and V. Galitski, *Phys. Rev. B* **87**, 235131 (2013).
- [13] T. Kitagawa, T. Oka, A. Brataas, L. Fu, and E. Demler, *Phys. Rev. B* **84**, 235108 (2011).
- [14] T. Oka and H. Aoki, *Phys. Rev. B* **79**, 081406 (2009).
- [15] P. Delplace, Á. Gómez-León, and G. Platero, *Phys. Rev. B* **88**, 245422 (2013).
- [16] Á. Gómez-León, P. Delplace, and G. Platero, *Phys. Rev. B* **89**, 205408 (2014).
- [17] L. Jiang, T. Kitagawa, J. Alicea, A. R. Akhmerov, D. Pekker, G. Refael, J. I. Cirac, E. Demler, M. D. Lukin, and P. Zoller, *Phys. Rev. Lett.* **106**, 220402 (2011).
- [18] A. Kundu and B. Seradjeh, *Phys. Rev. Lett.* **111**, 136402 (2013).
- [19] Á. Gómez-León and G. Platero, *Phys. Rev. Lett.* **110**, 200403 (2013).
- [20] M. S. Rudner, N. H. Lindner, E. Berg, and M. Levin, *Phys. Rev. X* **3**, 031005 (2013).
- [21] M. C. Rechtsman, J. M. Zeuner, Y. Plotnik, Y. Lumer, D. Podolsky, F. Dreisow, S. Nolte, M. Segev, and A. Szameit, *Nature (London)* **496**, 196 (2013).
- [22] Y. H. Wang, H. Steinberg, P. Jarillo-Herrero, and N. Gedik, *Science* **342**, 453 (2013).
- [23] M. Onoda, Y. Avishai, and N. Nagaosa, *Phys. Rev. Lett.* **98**, 076802 (2007).
- [24] J. Li, R.-L. Chu, J. K. Jain, and S.-Q. Shen, *Phys. Rev. Lett.* **102**, 136806 (2009).
- [25] C. W. Groth, M. Wimmer, A. R. Akhmerov, J. Tworzydło, and C. W. J. Beenakker, *Phys. Rev. Lett.* **103**, 196805 (2009).
- [26] Y. Xing, L. Zhang, and J. Wang, *Phys. Rev. B* **84**, 035110 (2011).
- [27] J. Song, H. Liu, H. Jiang, Q.-f. Sun, and X. C. Xie, *Phys. Rev. B* **85**, 195125 (2012).
- [28] F. D. M. Haldane, *Phys. Rev. Lett.* **61**, 2015 (1988).
- [29] See Supplemental Material at <http://link.aps.org/supplemental/10.1103/PhysRevLett.114.056801> for details of 6 sections. The first section provides definitions of Floquet theory; the second section introduces Floquet topological insulators; the third section provides a Born approximation treatment for disorder in this system; the fourth section provides details for calculating the Bott index for a disordered system; the fifth section shows finite size effects on the topological invariant as a function of quasienergy, and the sixth section provides details for the experimental realization in photonic lattices, which includes Refs. [30,31,34,35].
- [30] K. Kawano and T. Kitoh, *Introduction to Optical Waveguide Analysis* (Wiley, New York, 2001).
- [31] S. G. Johnson and J. D. Joannopoulos, *Opt. Express* **8**, 173 (2001).
- [32] T. A. Loring and M. B. Hastings, *Europhys. Lett.* **92**, 67004 (2010).
- [33] A. Szameit and S. Nolte, *J. Phys. B* **43**, 163001 (2010).
- [34] D. F. Martinez, *J. Phys. A* **36**, 9827 (2003).
- [35] N. H. Shon and T. Ando, *J. Phys. Soc. Jpn.* **67**, 2421 (1998).